Journal of Molecular Catalysis A: Chemical 370 (2013) 104–110

Contents lists available at SciVerse ScienceDirect

Journal of Molecular Catalysis A: Chemical

journal homepage: www.elsevier.com/locate/molcata

Molybdena–vanadia supported on alumina: Effective catalysts for the esterification reaction of acetic acid with *n*-butanol

Gheorghita Mitran, Octavian-Dumitru Pavel, Ioan-Cezar Marcu*

Laboratory of Chemical Technology and Catalysis, Department of Organic Chemistry, Biochemistry and Catalysis, Faculty of Chemistry, University of Bucharest, 4-12, Boulevard Regina Elisabeta, 030018 Bucharest, Romania

ARTICLE INFO

Article history:
Received 4 October 2012
Received in revised form
22 December 2012
Accepted 8 January 2013
Available online 19 January 2013

Keywords:
Esterification
Acetic acid
n-Butanol
n-Butyl acetate
Supported molybdena–vanadia catalysts

ABSTRACT

The paper describes the preparation of alumina-supported molybdena–vanadia catalysts, their structural and textural characterization using XRD, N_2 adsorption, UV–vis and NH_3-TPD techniques as well as their catalytic properties in the esterification reaction of acetic acid with *n*-butanol. The effects of esterification conditions including reaction time, catalyst loading and acid-to-alcohol mole ratio and of reactant pre-adsorption on the conversion were investigated. The catalytic activity correlated well with the number of strong acid sites which increased by increasing the vanadia content. In optimized conditions, conversions higher than 85% with 100% selectivity for *n*-butyl acetate can be obtained. Reactant pre-adsorption experiments suggested that the reaction follows the Langmuir–Hinshelwood mechanism. A good reusability of the catalysts after three reaction cycles was observed. A local interaction between molybdenum and vanadium on the catalyst surface has been evidenced.

1. Introduction

Nowadays, there is a great interest in the esterification reaction because organic esters are largely used in the production of plastic derivatives, perfumery, agro-chemistry and other branches of fine chemistry [1].

The *n*-butyl acetate is an important chemical having extensive applications in the industry being used in large quantities as a solvent in the lacquer industry and coating manufacture, extractant and dehydrator [1–3]. Additionally, it is able to replace the toxic and teratogenic ethoxy ethyl acetate, which is often used as a solvent [4]. The *n*-butyl acetate is commonly synthesized by esterification of acetic acid with *n*-butanol in the presence of strong acid catalysts, which is the most viable route for producing this value added product. Esterification being an equilibrium reaction, an excess of one reactant and/or continuously removing of water by adsorption on drying agents or by co-distillation with entrainers such as benzene or toluene can be used to enhance the performance of the reaction [3,5].

In last decade, numerous solid acid systems were used in esterification reactions, including classical solid acids such as ion-exchange resins [6–8], zeolites [9,10], superacids like sulfated zirconia [11,12], heteropoly acids (HPA) having the Keggin-type structure [13–16] but also oxides of elements with valence five or higher [17–19] and supported chlorides [20]. The commercially available solid acid catalysts have recently been comparatively studied in the esterification of acetic acid with butanol [21].

It is well known [22] that among the oxides of elements with valence five or higher, molybdena and vanadia present strong to very strong Brønsted acidity which make them good candidates as acid catalysts. The high surface area and good thermal stability of alumina could put together with their surface acidity leading to excellent solid acid catalysts. Indeed, it has recently been shown that alumina-supported molybdena and vanadia were able to catalyze the esterification reaction of acetic acid with *n*-butanol showing conversions of 81 and 63%, respectively, and 100% selectivity for *n*-butyl acetate at 100 °C and 2 h reaction time [23,24]. Nevertheless, while MoO_3/Al_2O_3 was stable during the catalytic reaction, a loss of the catalytic activity of the V_2O_5/Al_2O_3 was observed due to the leaching of vanadia from the alumina support. It is expected that the addition of MoO_3 to V_2O_5/Al_2O_3 will increase its surface acidity [25] and, consequently, its catalytic activity in the esterification reaction. Moreover, Mo and V could interact on the support surface [26,27] resulting in an increased catalyst stability. Hence, it is interesting to investigate MoO_3–V_2O_5/Al_2O_3 catalysts for the esterification reaction. To the best of our knowledge, there are no studies investigating alumina-supported MoO_3–V_2O_5 mixed oxides as catalysts for the esterification reaction in general and for the esterification of acetic acid with *n*-butanol in particular.

* Corresponding author.
E-mail addresses: ioancezar.marcu@g.unibuc.ro, ioancezar_marcu@yahoo.com (I.-C. Marcu).

1381-1169/$ – see front matter © 2013 Elsevier B.V. All rights reserved.
http://dx.doi.org/10.1016/j.molcata.2013.01.001

In the present contribution, we prepared γ-alumina-supported MoO_3–V_2O_5 catalysts with different loadings and Mo/V ratios and characterized them by several techniques, such as XRD, N_2 physisorption, NH_3-TPD and UV–vis diffuse reflectance spectroscopy. Their catalytic activity was examined by carrying out the esterification reaction of acetic acid with *n*-butanol under suitable conditions. Further, various reaction parameters such as effect of reaction time, temperature, molar ratio of the reactants were evaluated to optimize the reaction conditions.

2. Experimental

2.1. Catalysts preparation

Al_2O_3 support was prepared from $Al(NO_3)_3{\cdot}9H_2O$ (Fluka Analytical) by precipitation with ammonium carbonate (Lachema) at controlled pH of 6.5. Four different MoO_3–V_2O_5/Al_2O_3 catalysts with two MoO_3–V_2O_5 loadings, i.e. 5 and 10 wt%, and two MoO_3/V_2O_5 weight ratios, i.e. 9/1 and 1/9, were prepared using a one-step procedure. Thus, the two components were impregnated simultaneously by the incipient wetness method with an aqueous $(NH_4)_6Mo_7O_{24}{\cdot}4H_2O$ (Fluka Analytical) and NH_4VO_3 (Fluka Analytical) solution containing appropriate amounts of molybdenum and vanadium. After impregnation, the samples were dried in air at 100 °C and then calcined at 600 °C for 4 h. They were denoted $5Mo_9V_1Al$, $5Mo_1V_9Al$, $10Mo_9V_1Al$ and $10Mo_1V_9Al$, respectively.

2.2. Catalysts characterization

The crystalline phases were investigated by the X-ray diffraction (XRD) method. XRD patterns were obtained with a Philips PW 3710 type diffractometer equipped with a Cu K_α source (λ = 1.54 Å), operating at 50 kV and 40 mA. They were recorded over the 10–70° angular range with 0.02° (2θ) steps and an acquisition time of 1 s per point.

Surface areas of the catalysts were measured from the adsorption isotherms of nitrogen at −196 °C using the BET method with a Micromeritics ASAP 2020 sorptometer. Samples were out-gassed at 300 °C for 4 h in the degas port of the adsorption apparatus. The pore size distribution curves were calculated using the desorption branch of the isotherms with the Barrett–Joyner–Halenda (BJH) method.

The acidity of the catalysts was estimated by temperature-programmed desorption of ammonia (NH_3-TPD). About 0.1 g of the catalyst sample was dehydrated at 500 °C in dry air for 1 h and purged with N_2 for 0.5 h. The sample was then cooled down to 100 °C under the flow of N_2, and NH_3 was supplied to the sample until its saturation. For desorption of the physisorbed ammonia, a nitrogen stream was passed over the sample, at the same temperature, until no more NH_3 was observed in the exit flow. Finally, the chemisorbed NH_3 was desorbed in a N_2 flow by increasing the temperature successively up to 350 °C and 500 °C with a heating rate of 10 °C/min. The ammonia desorbed was bubbled through a solution of sulfuric acid. The acid in excess was titrated with a solution of NaOH, the amount of ammonia desorbed being then calculated. The ammonia desorbed at temperatures lower than 350 °C accounted for the weak and medium-strength acid sites while that desorbed in the temperature range from 350 to 500 °C, for the strong acid sites.

Diffuse reflectance UV–vis spectra were recorded in the range 200–650 nm, using Spectralon as a standard, in a Jasco V 670 spectrophotometer. The obtained reflectance spectra were converted into the dependencies of Kubelka–Munk function on the absorption energy.

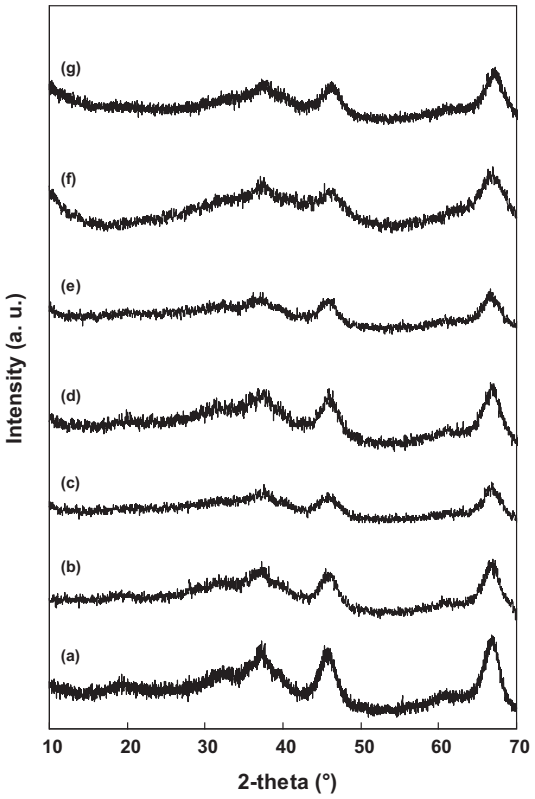

Fig. 1. X-ray diffraction patterns of the alumina support and of the alumina-supported MoO_3–V_2O_5 catalysts: (a) the alumina support, (b) $5Mo_9V_1Al$, (c) $5Mo_1V_9Al$, (d) $10Mo_9V_1Al$, (e) $10Mo_1V_9Al$, (f) $5Mo_9V_1Al$ used in three reaction cycles, and (g) $10Mo_1V_9Al$ used in three reaction cycles.

2.3. Catalytic test

The esterification reactions of acetic acid (Chimactiv, 99.5%) with *n*-butanol (Riedel-de Haën, 99.5%) were performed in a 150 mL two-neck flask equipped with a condenser and an additional port for sample withdrawal. The above assembly was heated using a thermostated hotplate. The reaction was carried out at 100 °C with a molar quantity of acetic acid of 0.09 and an *n*-butanol-to-acetic acid molar ratio varied from 1 to 3. Cyclohexane (Riedel-de Haën, 99.5%) was always added to the reaction mixture for water removal, the cyclohexane-to-acetic acid molar ratio being kept at 1. The amount of catalyst was varied between 0.5 and 1.3% of the mass of mixture charge in the reaction. All the experiments were conducted at a speed of agitation of 600 rpm to avoid diffusional limitations as reported elsewhere [23,24]. All the catalysts used in the reaction were in the powder form. Pre-adsorption experiments were performed by premixing the catalyst with one of the reactants or both at room temperature for 24 h followed by heating to 100 °C and charging the preheated remaining reactant. Samples from the organic layer were withdrawn at regular intervals and analyzed with a Thermo Finnigan chromatograph using a DB-5 column and a flame ionization detector. Under the employed conditions of reaction butyl acetate was the only product detected. The mass balances, calculated after a reaction time of 120 min, were always higher than 95%.

3. Results and discussion

3.1. Characterization of the catalysts

The X-ray diffraction measurements (Fig. 1) showed that the MoO_x–VO_x species are in all cases well dispersed on the support

Table 1
Physico-chemical properties of the catalysts.

Catalyst	BET surface area (m^2/g)	Pore volume (cm^3/g)	Number of acid sites (mmol/g)		
			Weak and medium	Strong	Total number
Al_2O_3	227	0.38	0.097	0.027	0.12
$5Mo_9V_1Al$	220	0.39	0.066	0.184	0.25
$10Mo_9V_1Al$	204	0.37	0.272	0.218	0.49
$5Mo_1V_9Al$	206	0.40	0.068	0.302	0.37
$10Mo_1V_9Al$	192	0.37	0.079	0.461	0.54

as only broad lines corresponding to γ-alumina (PDF 10-425) were observed. Neither V_2O_5 nor MoO_3 crystallites were detected at any MoO_x–VO_x loading on alumina. No major changes could be noted in the XRD patterns of the $5Mo_9V_1Al$ and $10Mo_1V_9Al$ catalysts after three reaction cycles (Fig. 1).

In general, the specific surface area and pore size of the catalyst have significant influence on its catalytic activity. The surface areas and pore volumes of the supported catalysts and of the alumina support were given in Table 1. After impregnation of alumina with MoO_3–V_2O_5 and by increasing the catalyst loading and V_2O_5 content, the surface area of the samples decreased. The reduction in surface area has already been observed for alumina-supported molybdena–vanadia [28] and may be due to the blockage of pores by MoO_x–VO_x species. Nevertheless, the supported samples possess high surface areas due to the dispersion effect of porous carrier. All the catalysts displayed typical type IV nitrogen adsorption/desorption isotherms (according to IUPAC classification) with a clear hysteresis loop at the relative pressure of 0.5–0.85, characteristic of mesoporous materials with uniform cylindrical pores [29], as exemplified in Fig. 2a for $5Mo_9V_1Al$ and $10Mo_1V_9Al$ catalysts. The catalysts show uniform and narrow pore size distributions with average peak pore diameters in the range 5–9 nm (Fig. 2b) and, therefore, they should be readily accessible to the reactants. No correlation can be made between the average pore diameter and the catalyst loading.

Surface acidity is the most important function of the catalysts used in the esterification reaction. Therefore, the total acidities of the catalysts, expressed as the total number of acid sites per gram of catalyst, have been determined by NH_3-TPD and are presented in Table 1. It can be observed that the total acidity increased by adding MoO_3–V_2O_5 to alumina and by increasing the MoO_3–V_2O_5 loading and that at similar MoO_3–V_2O_5 loadings, it was higher for the samples with higher vanadia content, following the order: $Al_2O_3 < 5Mo_9V_1Al < 5Mo_1V_9Al < 10Mo_9V_1Al < 10Mo_1V_9Al$. Nevertheless, the number of strong acid sites increased continuously with the vanadia content following the order: $Al_2O_3 < 5Mo_9V_1Al < 10Mo_9V_1Al < 5Mo_1V_9Al < 10Mo_1V_9Al$. This suggests that the strong acid sites are mainly associated to the presence of vanadia.

The UV–vis diffuse reflectance spectra of the catalysts are comparatively shown in Fig. 3. V_2O_5/Al_2O_3 and MoO_3/Al_2O_3 with 10 wt% metal oxide loading were used as reference samples. The spectrum of V_2O_5/Al_2O_3 sample shows five main absorption bands at about 220, 260, 340, 380 and 480 nm. The 220 and 260 nm bands can be assigned to isolated tetrahedrally coordinated V^{5+} species, while the 340 and 380 nm bands can be attributed to isolated octahedrally coordinated V^{5+} species. The 480 nm band can be associated to octahedral VO_6 chains from well dispersed or crystalline V_2O_5 clusters [30,31]. In the V_2O_5/Al_2O_3 sample crystalline V_2O_5 has been evidenced [24]. The spectrum of MoO_3/Al_2O_3 sample shows three main absorption bands at about 220, 260 and 300 nm. The 220 nm and 260 nm bands can be attributed to the tetrahedral molybdate species, whereas the 300 nm band can be assigned to the octahedral molybdate species [32–34]. By adding molybdena and decreasing the vanadia content in the V_2O_5–MoO_3/Al_2O_3 samples, the 480 and 380 nm bands disappear while the 340 nm band fall in the range 330–310 nm. These results suggest that, on one hand, the isolated and polymerized octahedral VO_6 species decrease then disappear by decreasing the vanadia content from 10 wt% in V_2O_5/Al_2O_3 sample to 0.5 wt% in $5Mo_9V_1Al$ sample [35] and, on the other hand, an interaction between molybdenum and

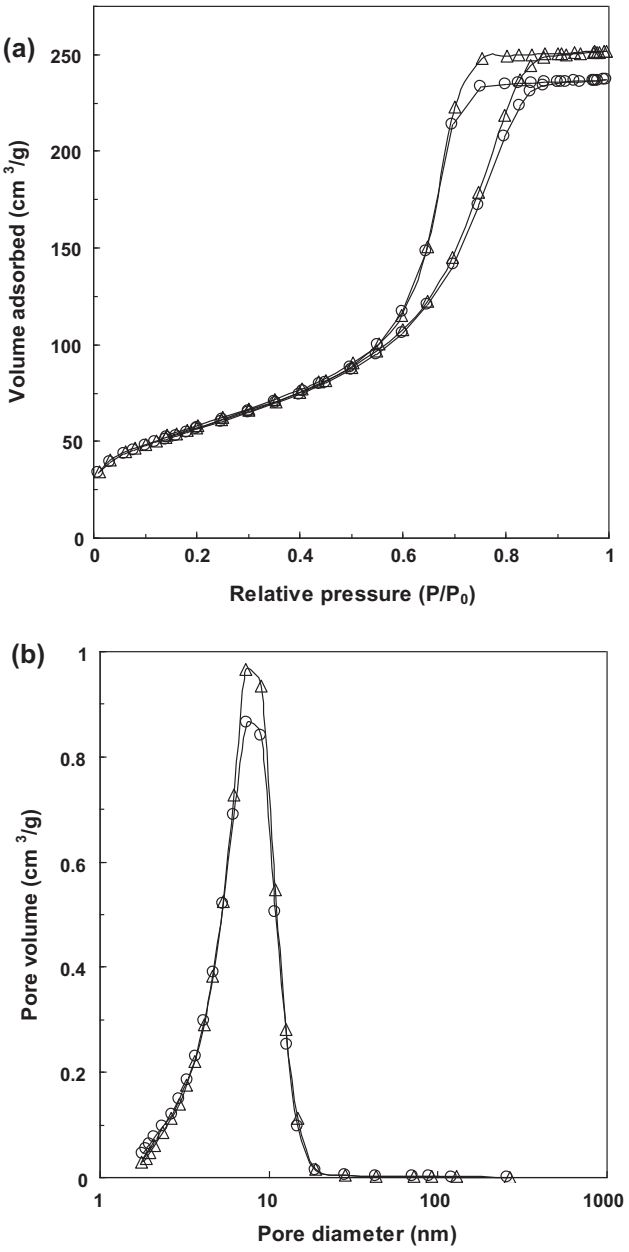

Fig. 2. N_2 adsorption–desorption isotherms (a) and pore size distribution curves (b) of $5Mo_9V_1Al$ (△) and $5Mo_1V_9Al$ (○) catalysts.

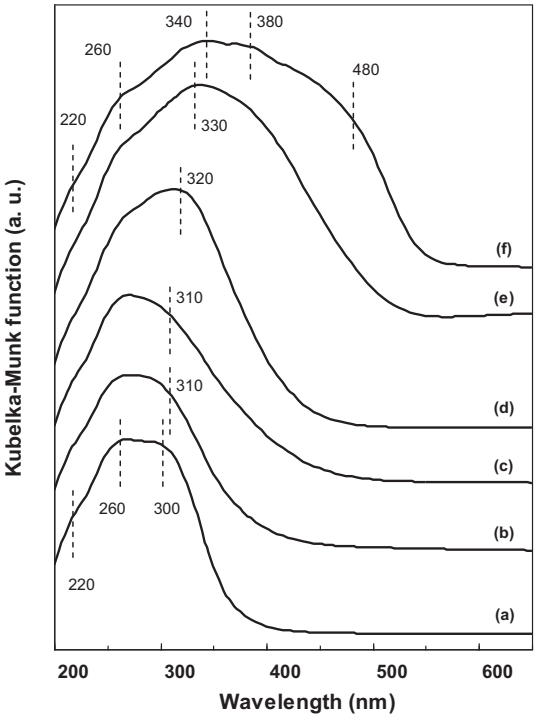

Fig. 3. UV–vis diffuse reflectance spectra of the MoO_3–V_2O_5/Al_2O_3 catalysts and of the V_2O_5/Al_2O_3 and MoO_3/Al_2O_3 reference materials: (a) MoO_3/Al_2O_3, (b) $5Mo_9V_1Al$, (c) $10Mo_9V_1Al$, (d) $5Mo_1V_9Al$, (e) $10Mo_1V_9Al$, and (f) V_2O_5/Al_2O_3.

vanadium takes place with characteristic bands at 310–330 nm as already shown by Volta and coworkers [27].

3.2. Catalytic activity

The effects of esterification conditions including reaction time, catalyst loading and acid-to-alcohol mole ratio and of reactant pre-adsorption on the reaction conversion were investigated, the results obtained being presented below.

3.2.1. Effect of reaction time

The influence of the reaction time was studied in the following reaction conditions: *n*-butanol-to-acetic acid mole ratio 2:1, the catalyst representing 0.7 wt% of the mass of mixture charge in the reaction and the reaction temperature being kept at 100 °C. In these conditions, the selectivity of *n*-butyl acetate being, in all cases, 100%, the conversion of acetic acid can represent the yield of *n*-butyl acetate. The results obtained are shown in Fig. 4a. As expected, for all the catalysts and support a gradual rise in the conversion with increasing in duration of the reaction period can be observed. The activity of the different catalysts and the support at 120 min reaction time ranged as follows (the conversion of acetic acid in parenthesis): Al_2O_3 (41%) < $5Mo_9V_1Al$ (46%) < $10Mo_9V_1Al$ (62.5%) < $5Mo_1V_9Al$ (68.3%) < $10Mo_1V_9Al$ (71%). This order is similar to that corresponding to the number of strong acid sites suggesting that they play a key role in the esterification reaction of acetic acid with *n*-butanol. The conversion values observed for the best catalysts in the series studied are comparable with those reported for the same reaction performed with commercially available catalysts [21]. It is noteworthy that, by adding low quantities of molybdena to γ-alumina-supported vanadia, the catalytic activity was improved as the acetic acid conversions for $5Mo_1V_9Al$ and $10Mo_1V_9Al$ catalysts were higher compared with V_2O_5/Al_2O_3 with similar vanadia contents, i.e. 5 and 10 wt%, tested in similar reaction conditions, for which the acetic acid conversions were 50.3 and 66.4%, respectively [24].

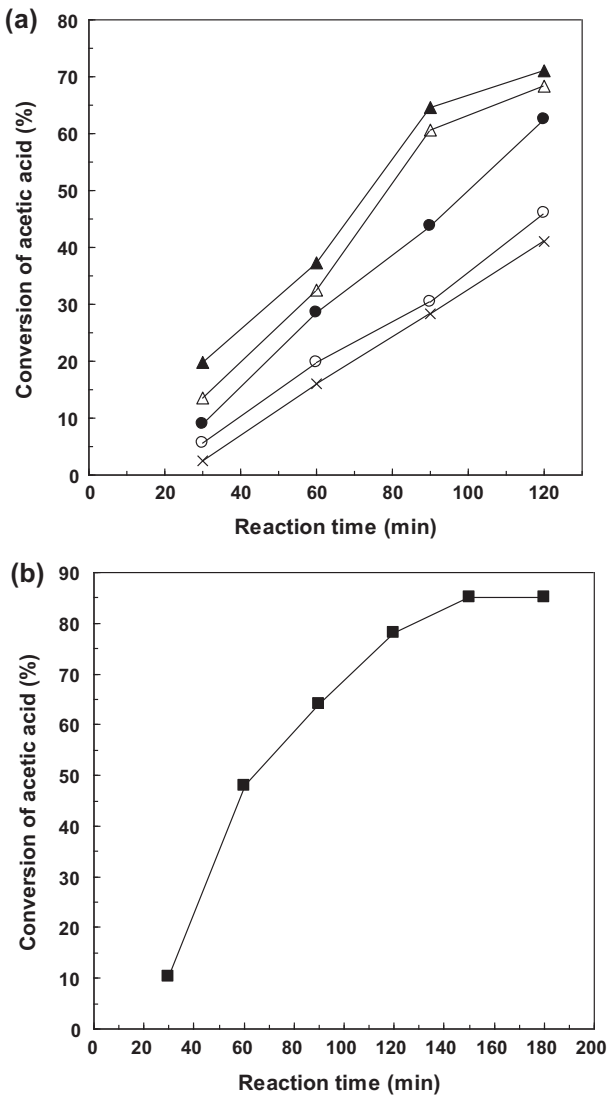

Fig. 4. Conversion of acetic acid as a function of the reaction time: (a) on the different catalysts with a *n*-butanol-to-acetic acid mole ratio 2:1, 0.7 wt% catalyst and reaction temperature 100 °C (× – alumina support; ○ – $5Mo_9V_1Al$; ● – $10Mo_9V_1Al$; △ – $5Mo_1V_9Al$; ▲ – $10Mo_1V_9Al$) and (b) on the $10Mo_9V_1Al$ catalyst with a *n*-butanol-to-acetic acid mole ratio 3:1, 1 wt% catalyst and reaction temperature 100 °C.

For the $10Mo_9V_1Al$ catalyst in optimized conditions, i.e. *n*-butanol-to-acetic acid mole ratio 3:1, the catalyst representing 1 wt% of the mass of mixture charge in the reaction and the reaction temperature being kept at 100 °C, the reaction time was increased until reaching constant conversion (Fig. 4b). The conversion reached a maximum of ca. 85% with 100% selectivity of *n*-butyl acetate after 150 min of reaction, and then it remained almost unchanged. This suggests that 150 min is the optimum reaction time. Note that it was lower than that reported for other supported catalysts, such as supported silicotungstic acid [15], supported dodecatungstophosphoric acid [16] and supported niobia [17], but comparable with that reported for the commercially available ion-exchange resins [21] tested in the same reaction.

3.2.2. Effect of reactant pre-adsorption

Two types of mechanisms can be considered for the esterification reaction over solid acid catalysts: one involving the surface reaction between a chemisorbed species and a species from the

liquid phase, known as Eley–Rideal type mechanism, and other requiring the chemisorption of both acid and alcohol, known as Langmuir–Hinshelwood type mechanism. Pre-adsorption of alcohol, acid or both alcohol and acid on the solid catalyst before the esterification reaction can give information about the mechanism involved [36]. Thus, the effect of reactant pre-adsorption has been studied with the $5Mo_9V_1Al$ catalyst for a *n*-butanol-to-acetic acid mole ratio of 1:1 and with 0.7 wt% catalyst. It has been premixed with acetic acid, *n*-butanol or both acetic acid and *n*-butanol for 24 h at room temperature and then heated until reaching the reaction temperature, i.e. 100 °C. At this moment the preheated remaining reactant was added. The obtained conversion versus time curves are shown in Fig. 5 where the curve corresponding to the reaction without premixing of reactants is also presented for comparison. It can be observed that the highest conversion values where obtained when premixing the catalyst with the mixture of acetic acid and *n*-butanol. The conversion of acetic acid decreased following the order: premixing with both acetic acid and *n*-butanol > no premixing > premixing with acetic acid > premixing with *n*-butanol. These results suggest that the esterification reaction needs the chemisorption of both acetic acid and *n*-butanol and involves a Langmuir–Hinshelwood type mechanism. This result was in disagreement with those obtained by Parida et al. for the

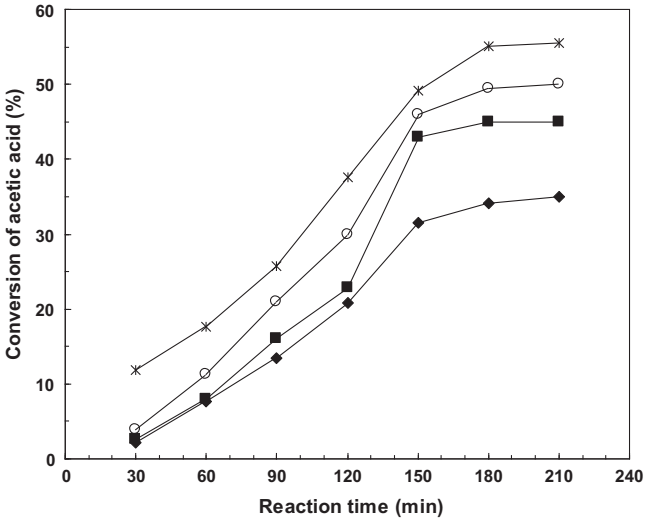

Fig. 5. The effect of reactant pre-adsorption on the $5Mo_9V_1Al$ catalyst with a *n*-butanol-to-acetic acid mole ratio of 1:1, 0.7 wt% catalyst and reaction temperature 100 °C: (○) no pre-adsorption, (■) pre-adsorption of acetic acid, (♦) pre-adsorption of *n*-butanol, and (*) pre-adsorption of both acetic acid and *n*-butanol.

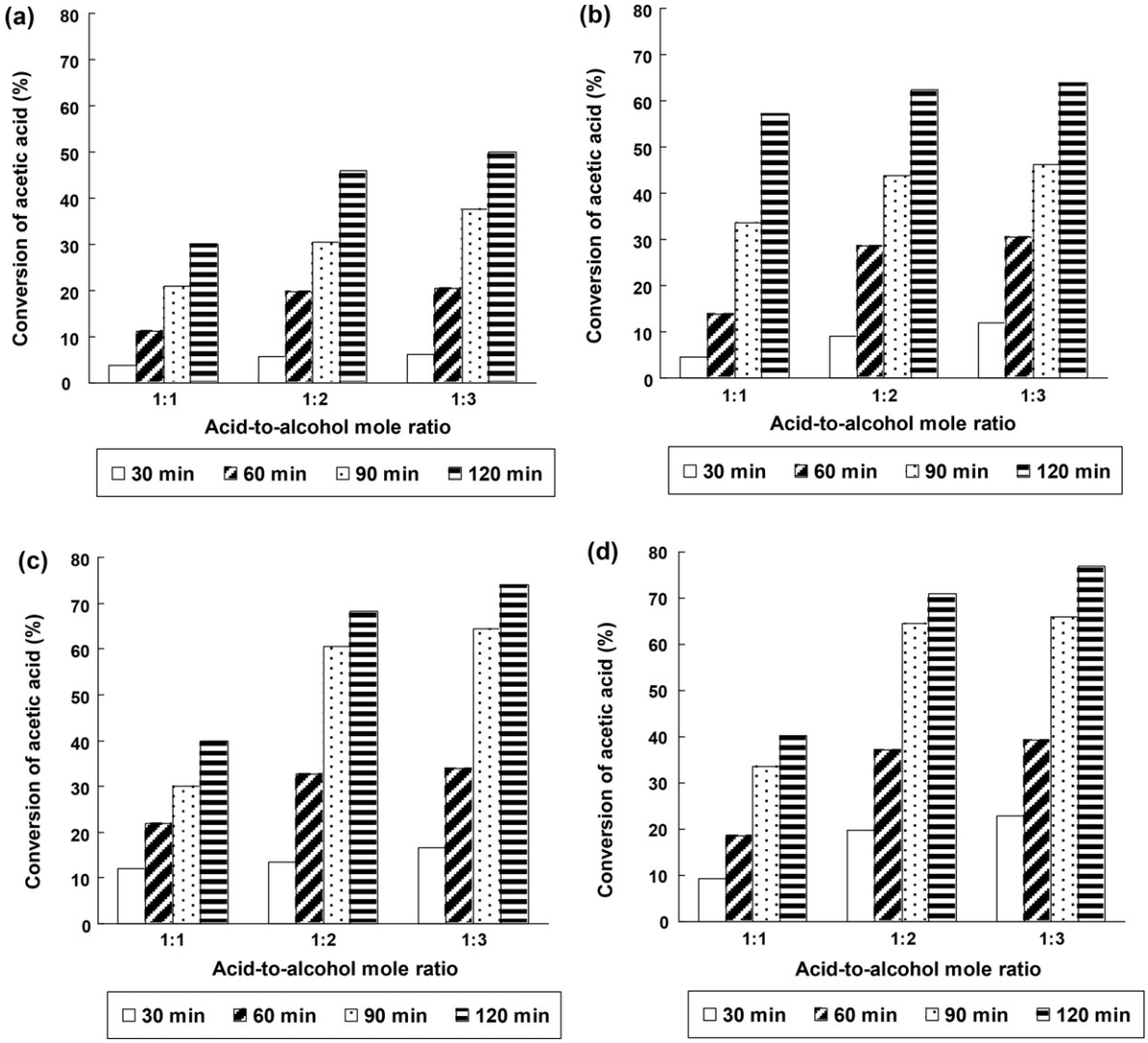

Fig. 6. Effect of acid-to-alcohol mole ratio on the esterification of acetic acid with *n*-butanol using (a) $5Mo_9V_1Al$, (b) $10Mo_9V_1Al$, (c) $5Mo_1V_9Al$ and (d) $10Mo_1V_9Al$ as catalysts. Reaction conditions: temperature 100 °C, 0.7 wt% catalyst.

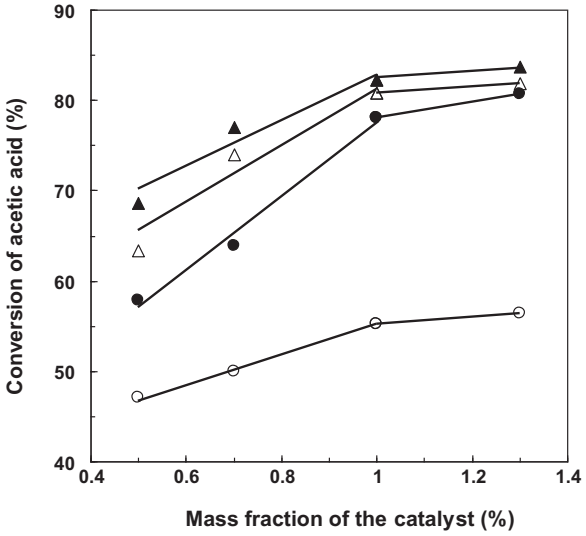

Fig. 7. Effect of catalyst concentration on the esterification of acetic acid with *n*-butanol using $5Mo_9V_1Al$ (○), $10Mo_9V_1Al$ (●), $5Mo_1V_9Al$ (△) and $10Mo_1V_9Al$ (▲) as catalysts. Reaction conditions: temperature 100 °C, acetic acid-to-*n*-butanol molar ratio 1:3 and reaction time 120 min.

esterification of acetic acid with *n*-butanol catalyzed by silicotungstic acid supported zirconia [15] or vanadium phosphate [37] and by Liu et al. [38] for the silica-supported Nafion-catalyzed esterification of acetic acid with methanol. However, our result agrees with that obtained by Lee et al. [39], Teo and Saha [40] and Akbay and Altıokka [41] for the esterification of acetic acid with amyl alcohol catalyzed by acid resin catalysts and by Miao and Shanks [36] for the esterification of acetic acid with methanol over sulfonic acid-functionalized mesoporous silica.

It is noteworthy that the results above also showed that the chemisorption of *n*-butanol was stronger than that of acetic acid as the conversion values obtained by premixing the catalyst with *n*-butanol were lower than those obtained by premixing the catalyst with acetic acid. This is in line with other literature results proposing a stronger chemisorption of the alcohol than the acid [40,42]. Moreover, it can be observed that the pre-adsorption of either acetic acid or *n*-butanol inhibited the reaction suggesting a competitive adsorption of the reactants on the catalyst surface.

3.2.3. Effect of initial reactants molar ratio

The initial acid-to-alcohol molar ratio was varied from 1:1 to 1:3 for the reaction at 100 °C and with 0.7 wt% catalyst, the results obtained being showed in Fig. 6. It can be observed that, as expected, for all the catalysts studied and for all the reaction times considered, the conversion substantially increased by increasing the initial acid-to-alcohol mole ratio from 1:1 to 1:2. By further increasing the acid-to-alcohol mole ratio to 1:3, the conversion increased but to a lower extent. This could be explained by a competitive adsorption of acetic acid and *n*-butanol, with a stronger adsorption of the alcohol in agreement with the adsorption behavior described earlier. Note that the selectivity for *n*-butyl acetate was, in all cases, 100% and the conversion of acetic acid reached 77% in the presence of $10Mo_1V_9Al$ catalyst for an acetic acid-to-*n*-butanol mole ratio equal to 1:3 and a reaction time of 120 min.

3.2.4. Influence of catalyst amount

The amount of the catalyst was varied from 0.5 to 1.3% by mass of the total reaction mixture using $5Mo_9V_1Al$, $10Mo_9V_1Al$, $5Mo_1V_9Al$ and $10Mo_1V_9Al$ as catalysts, while keeping the *n*-butanol-to-acetic acid mole ratio at 3:1, the reaction temperature at 100 °C and the reaction time at 120 min (Fig. 7). In all cases, the conversion of acetic acid increased with increasing the catalyst amount from 0.5 to ca. 1% and then it tends to a plateau. This suggests that 1 wt% is the optimal mass fraction of the catalyst in the reaction medium.

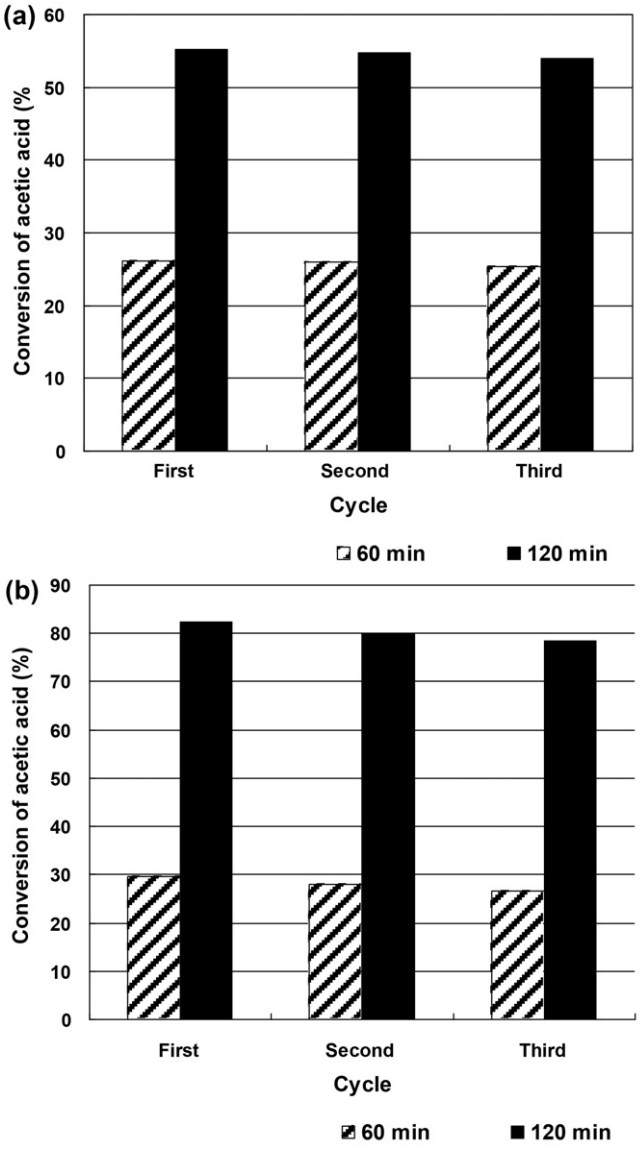

Fig. 8. Reusability of the (a) $5Mo_9V_1Al$ and (b) $10Mo_1V_9Al$ catalysts in the esterification of acetic acid with *n*-butanol. Reaction conditions: temperature 100 °C, acetic acid-to-*n*-butanol molar ratio 1:3 and 1 wt% catalyst.

3.2.5. Reusability of the catalyst

Compared with homogeneous acids, the advantages of solid acid catalysts are their easy recovery and good reusability. Therefore, it is quite necessary to evaluate the reusability of the alumina-supported molybdena–vanadia catalysts, especially in viewpoint of practical application. The $5Mo_9V_1Al$ and $10Mo_1V_9Al$ catalysts were used for recycling experiments carried out under the following reaction conditions: acetic acid-to-*n*-butanol mole ratio was 1:3, 1 wt% catalyst, reaction temperature 100 °C. In order to regenerate the catalyst after 2 h of reaction, it was separated by filtration, washed with distilled water several times, dried at 120 °C in air and then used in the esterification reaction with a fresh reaction mixture. For the regenerated $5Mo_9V_1Al$ and $10Mo_1V_9Al$ catalysts after three cycles, the conversion decreased by ca. 1% and 4%, respectively (Fig. 8), suggesting a good reusability of these catalysts in the esterification of acetic acid with *n*-butanol. It is noteworthy that,

compared with the alumina-supported vanadia catalyst with a similar vanadia content, i.e. 10 wt%, for which the conversion decreased by 15% after three reaction cycles [24], the $10Mo_1V_9Al$ catalyst had a much better stability. This suggests indeed that molybdena and vanadia interact on the catalyst surface increasing the catalyst stability [26]. Additionally, based on the DR–UV–Vis results, the polymerized VO_6 species present on the catalyst surface seem, in particular, to be responsible for the catalyst instability during the catalytic test.

4. Conclusion

MoO_3–V_2O_5 catalysts supported on γ-alumina act as efficient and stable solid acid catalysts for the esterification of acetic acid with *n*-butanol. The catalytic activity correlated well with the number of strong acid sites which increased by increasing the vanadia content. It ranged as follows (the conversion of acetic acid at 120 min reaction time in parenthesis): Al_2O_3 (41%) < $5Mo_9V_1Al$ (46%) < $10Mo_9V_1Al$ (62.5%) < $5Mo_1V_9Al$ (68.3%) < $10Mo_1V_9Al$ (71%). In all the esterification reactions the selectivity for butyl acetate was 100%. Reactant pre-adsorption experiments suggested that the reaction follows the Langmuir–Hinshelwood mechanism with a stronger adsorption of *n*-butanol than acetic acid.

The optimum reaction time was about 150 min and the optimal mass fraction of the catalyst in the reaction medium was found to be around 1 wt%. A good reusability of the catalysts after three reaction cycles was observed. A local interaction between molybdenum and vanadium on the catalyst surface has been evidenced. Compared with V_2O_5/Al_2O_3 with similar vanadia loadings, the MoO_3–V_2O_5/Al_2O_3 catalysts showed not only an increased stability during the esterification reaction, but also an improved catalytic activity.

References

[1] Kirk-Othmer, Encyclopedia of Chemical Technology, vol. 9, fourth ed., John Wiley & Sons, New York, 1994, p 797.
[2] G.B. Varadwaj, K.M. Parida, Catal. Lett. 141 (2011) 1476–1483.
[3] S. Blagov, S. Parada, O. Bailer, P. Moritz, D. Lam, R. Weinand, H. Hasse, Chem. Eng. Sci. 61 (2006) 753–765.
[4] S. Steinigeweg, J. Gmehling, Ind. Eng. Chem. Res. 41 (2002) 5483–5490.
[5] E. Ameri, A. Moheb, S. Roodpeyma, Korean J. Chem. Eng. 28 (2011) 1593–1598.
[6] M.J. Lee, J.Y. Chiu, H.M. Lin, Ind. Eng. Chem. Res. 41 (2002) 2882–2887.
[7] M.R. Altıokka, A. Citak, Appl. Catal. A 239 (2003) 141–148.
[8] A. Izci, F. Bodur, React. Funct. Polym. 67 (2007) 1458–1464.
[9] I. Hoek, T.A. Nijhuis, A.I. Stankiewich, J.A. Moulijn, Appl. Catal. A 266 (2004) 109–116.
[10] S.R. Kirumakki, N. Nagaraju, S. Narayanan, Appl. Catal. A 273 (2004) 1–9.
[11] S. Ardizzone, C.L. Bianchi, V. Ragaini, B. Vercelli, Catal. Lett. 62 (1999) 59–65.
[12] S. Khire, P.V. Bhagwat, M. Fernandes, P.B. Gangundi, H. Vadalia, Indian J. Chem. Technol. 19 (2012) 342–350.
[13] J.H. Sepúlveda, J.C. Yori, C.R. Vera, Appl. Catal. A 288 (2005) 18–24.
[14] F. Zhang, J. Wang, C. Yuan, X. Ren, Sci. China: Ser. B Chem. 49 (2006) 140–147.
[15] K.M. Parida, S. Mallick, J. Mol. Catal. A 275 (2007) 77–83.
[16] S.K. Bhorodwaj, M.G. Pathak, D.K. Dutta, Catal. Lett. 133 (2009) 185–191.
[17] V.S. Braga, I.C.L. Barros, F.A.C. Garcia, S.C.L. Dias, J.A. Dias, Catal. Today 133–135 (2008) 106–112.
[18] A.A. Costa, P.R.S. Braga, J.L. de Macedo, J.A. Dias, S.C.L. Dias, Micropor. Mesopor. Mater. 147 (2012) 142–148.
[19] Y.-M. Park, S.-H. Chung, H.J. Eom, J.-S. Lee, K.-Y. Lee, Biores. Technol. 101 (2010) 6589–6593.
[20] M. Salavati-Niasari, T. Khosousi, S. Hydarzadeh, J. Mol. Catal. A 235 (2005) 150–153.
[21] T.A. Peters, N. Benes, A. Holmen, J. Keurentjes, Appl. Catal. A 297 (2006) 182–188.
[22] G. Busca in, J.L.G. Fierro (Eds.), Metal Oxides: Chemistry and Applications, CRC Press, Boca Raton, 2006 (chapter 9).
[23] G. Mitran, É. Makó, Á. Rédey, I.C. Marcu, Catal. Lett. 140 (2010) 32–37.
[24] G. Mitran, É. Makó, Á. Rédey, I.C. Marcu, CR Chim. 15 (2012) 793–798.
[25] N. Haddad, E. Bordes-Richard, L. Hilaire, A. Barama, Catal. Today 126 (2007) 256–263.
[26] M.A. Bañares, S.J. Khatib, Catal. Today 96 (2004) 251–257.
[27] M. Roy, H. Ponceblanc, J.C. Volta, Top. Catal. 11/12 (2000) 101–109.
[28] B. Mitra, I.E. Wachs, G. Deo, J. Catal. 240 (2006) 151–159.
[29] K.S.W. Sing, D.H. Everett, R.A.W. Haul, L. Moscou, R.A. Pierotti, J. Rouquerol, T. Siemieniewska, Pure Appl. Chem. 57 (1985) 603–619.
[30] E.V. Kondratenko, M. Baerns, Appl. Catal. A 222 (2001) 133–143.
[31] G. Centi, S. Perathoner, F. Trifiró, A. Aboukais, C.F. Aïssi, M. Guelton, J. Phys. Chem. 96 (1992) 2617–2629.
[32] A. Duan, G. Wan, Z. Zhao, C. Xu, Y. Zheng, Y. Zhang, T. Dou, X. Bao, K. Chung, Catal. Today 119 (2007) 13–18.
[33] H. Aritani, T. Tanaka, T. Funabiki, S. Yoshida, K. Eda, N. Sotani, M. Kudo, S. Hasegawa, J. Phys. Chem. 100 (1996) 19495–19501.
[34] M.C. Abello, M.F. Gomeza, O. Ferretti, Appl. Catal. A 207 (2001) 421–431.
[35] E.F. Aboelfetoh, R. Pietschnig, Catal. Lett. 127 (2009) 83–94.
[36] S. Miao, B.H. Shanks, J. Catal. 279 (2011) 136–143.
[37] K.M. Parida, G.C. Behera, Catal. Lett. 140 (2010) 197–204.
[38] Y.J. Liu, E. Lotero, J.G. Goodwin, J. Catal. 242 (2006) 278–286.
[39] M.J. Lee, H.T. Wu, H.M. Lin, Ind. Eng. Chem. Res. 39 (2000) 4094–4099.
[40] H.T.R. Teo, B. Saha, J. Catal. 228 (2004) 174–182.
[41] E.Ö. Akbay, M.R. Altıokka, Appl. Catal. A 396 (2011) 14–19.
[42] M.T. Sanz, R. Murga, S. Beltran, J.L. Cabezas, J. Coca, Ind. Eng. Chem. Res. 41 (2002) 512–517.